New Phytologist

Research

Ocean acidification decreases the light-use efficiency in an Antarctic diatom under dynamic but not constant light

Clara J. M. Hoppe[1], Lena-Maria Holtz[1], Scarlett Trimborn[1,2] and Björn Rost[1]

[1]Alfred Wegener Institute – Helmholtz Centre for Polar and Marine Research, Am Handelshafen 12, Bremerhaven 27570, Germany; [2]University Bremen, Leobener Straße NW2-A, Bremen 28359, Germany

Author for correspondence:
Clara J. M. Hoppe
Tel: +49 471 4831 2096
Email: Clara.Hoppe@awi.de

Received: *16 September 2014*
Accepted: *12 January 2015*

New Phytologist (2015)
doi: 10.1111/nph.13334

Key words: *Chaetoceros debilis*, CO_2, multiple stressors, photophysiology, phytoplankton, primary production, Southern Ocean.

Summary

- There is increasing evidence that different light intensities strongly modulate the effects of ocean acidification (OA) on marine phytoplankton. The aim of the present study was to investigate interactive effects of OA and dynamic light, mimicking natural mixing regimes.
- The Antarctic diatom *Chaetoceros debilis* was grown under two pCO_2 (390 and 1000 μatm) and light conditions (constant and dynamic), the latter yielding the same integrated irradiance over the day. To characterize interactive effects between treatments, growth, elemental composition, primary production and photophysiology were investigated.
- Dynamic light reduced growth and strongly altered the effects of OA on primary production, being unaffected by elevated pCO_2 under constant light, yet significantly reduced under dynamic light. Interactive effects between OA and light were also observed for Chl production and particulate organic carbon quotas.
- Response patterns can be explained by changes in the cellular energetic balance. While the energy transfer efficiency from photochemistry to biomass production ($\Phi_{e,C}$) was not affected by OA under constant light, it was drastically reduced under dynamic light. Contrasting responses under different light conditions need to be considered when making predictions regarding a more stratified and acidified future ocean.

Introduction

The Southern Ocean (SO) plays a pivotal role in the global carbon cycle (Marinov *et al.*, 2006), strongly influencing atmospheric CO_2 concentrations on glacial–interglacial timescales (Moore *et al.*, 2000; Sigman *et al.*, 2010). Today, the SO takes up 15–40% of the anthropogenic CO_2 (Khatiwala *et al.*, 2009), a large proportion of which is mediated by phytoplankton, in particular diatoms (Nelson *et al.*, 1995; Takahashi *et al.*, 2002). The potential for carbon sequestration via the biological pump (Volk & Hoffert, 1985) is, however, restricted through iron and light limitation (Martin, 1990; Moore *et al.*, 2007; Feng *et al.*, 2010). Regarding the latter, deep vertical mixing induced by strong winds leads to pronounced changes in the light regime as well as low integrated irradiances that phytoplankton cells encounter in the upper mixed layer (MacIntyre *et al.*, 2000).

Diatoms tend to dominate under well-mixed, nutrient-rich environments where light is the main factor controlling growth rates (Sarthou *et al.*, 2005). Even though diatom species were found to differ in their photophysiological characteristics, this group can generally be characterized by high photochemical efficiencies, low susceptibilities towards photoinhibition, and high plasticity in photoacclimation (Wagner *et al.*, 2006; Lavaud *et al.*, 2007; Kropuenske *et al.*, 2009; Su *et al.*, 2012; Li & Campbell, 2013). Overall, diatoms seem to be less compromised by fluctuating irradiances than other phytoplankton groups (van Leeuwe *et al.*, 2005; Wagner *et al.*, 2006; Lavaud *et al.*, 2007; Jin *et al.*, 2013). These physiological features can, to a large degree, explain the dominance of diatoms in natural phytoplankton assemblages exposed to deep-mixing regimes like the SO (Sarthou *et al.*, 2005). Studies investigating the effects of dynamic light on diatoms often showed that while C : N ratios stayed constant, photosynthetic efficiencies increased and growth rates decreased compared with constant light regimes (e.g. van Leeuwe *et al.*, 2005; Wagner *et al.*, 2006; Kropuenske *et al.*, 2009; Mills *et al.*, 2010; Shatwell *et al.*, 2012). This indicates increased costs imposed by continuous photoacclimation and/or time spent under nonoptimal configuration of the core physiological apparatus. Despite these general trends, large differences in the magnitude of responses were observed between studies. These could be caused by differences in environmental conditions (e.g. temperatures, nutrient concentrations, seawater carbonate chemistry), which may modulate phytoplankton cells' ability to cope with fluctuating light fields (Jin *et al.*, 2013).

Owing to the high solubility of CO_2 under low water temperatures (Sarmiento *et al.*, 2004), the effects of increased CO_2 concentrations and decreased pH on SO phytoplankton have gained increasing attention in recent years (Tortell *et al.*, 2008; Feng *et al.*, 2010; Boelen *et al.*, 2011; Hoogstraten *et al.*, 2012a,b; Hoppe *et al.*, 2013; Trimborn *et al.*, 2013). The observed sensitivity of phytoplankton to these changes, commonly referred to as

Ocean Acidification (OA), can be partially attributed to beneficial effects of an increased supply of CO_2. The carbon-fixing enzyme RubisCO has a poor affinity for CO_2, with half-saturation constants (K_M) being higher than the current concentrations of aquatic CO_2 (Badger *et al.*, 1998). To overcome substrate limitation arising from this, phytoplankton employ so-called carbon concentrating mechanisms (CCMs), which increase the CO_2 concentration at the reactive site of RubisCO (Reinfelder, 2011). CCMs of diatoms include active CO_2 and HCO_3^- uptake, C_4-like pathways in some species, as well as the expression of carbonic anhydrase, which accelerates the inter-conversion of CO_2 and HCO_3^- (Morel *et al.*, 1994; Reinfelder *et al.*, 2000; Burkhardt *et al.*, 2001). Even though CCMs of diatoms were found to be highly efficient in preventing carbon limitation under most conditions (e.g. Badger *et al.*, 1998; Hopkinson *et al.*, 2011; Trimborn *et al.*, 2013), they are also commonly down-regulated under higher external CO_2 availability, lowering the overall metabolic costs of carbon acquisition under OA (Burkhardt *et al.*, 2001; Rost *et al.*, 2003; Trimborn *et al.*, 2008).

Results regarding the CO_2 sensitivity in primary production of diatom-dominated phytoplankton assemblages as well as isolated strains of the SO vary greatly between studies, indicating little to high potential for 'CO_2 fertilization' (e.g. Tortell *et al.*, 2008; Feng *et al.*, 2010; Boelen *et al.*, 2011; Hoppe *et al.*, 2013; Trimborn *et al.*, 2014). Such differences in OA responses can be explained by intra- and interspecific variability (Langer *et al.*, 2009; Trimborn *et al.*, 2013), but also by deviating experimental conditions. Besides the impact of temperature (Tatters *et al.*, 2013) and nutrient availability (Hoppe *et al.*, 2013), the effect of light intensities on OA responses has been shown to be particularly important (Kranz *et al.*, 2010; Ihnken *et al.*, 2011; Gao *et al.*, 2012a). In the coccolithophore *Emiliania huxleyi*, for example, the CO_2 sensitivity of carbon fixation and calcification was greatly enhanced under low vs high light (Rokitta & Rost, 2012). Several studies on diatoms have shown, furthermore, an increased susceptibility towards photoinhibition under elevated pCO_2 concentrations (Wu *et al.*, 2010; McCarthy *et al.*, 2012; Li & Campbell, 2013). Even though all of these studies increased our knowledge on the interactive effects between OA and light intensities, the transferability to processes in the ocean, where light intensities are highly dynamic, is questionable.

Regarding the potential interaction of OA and light regimes, there are only limited data in existence. Boelen *et al.* (2011) did not observe significant effects of pCO_2 concentrations up to 750 µatm under either constant or dynamic light for the Antarctic diatom *Chaetoceros brevis*. In the coccolithophore *Gephyrocapsa oceanica*, however, the combination of a pCO_2 of 1000 µatm and short-term (2 h) exposure to dynamic light led to lowered carbon fixation compared with ambient pCO_2 and constant light (Jin *et al.*, 2013). In view of these conflicting results, a mechanistic understanding of the complex interactions between OA and dynamic light is required. As changes in light harvesting need to be balanced by the sum of all downstream processes, it is particularly important to focus on the interplay between the involved processes and their respective timescales. For example, comparing the short-term evolution of O_2 and production of energy carriers and reductive equivalents (ATP and NADPH) with the biomass build-up or growth on longer timescales clearly shows that both 'ends of photosynthesis' do not always match (Behrenfeld *et al.*, 2008). Changes in environmental conditions, such as light regime or carbonate chemistry, will inevitably impact the balance of cellular processes, affecting the energy transfer efficiency of photosynthetic light harvesting to carbon fixation (Wagner *et al.*, 2006; Rokitta & Rost, 2012).

In view of such considerations and earlier findings on the isolated effects of OA and dynamic light, the goal of the present study was to investigate how the energy transfer efficiency from photochemistry to biomass build-up and growth is affected by the interaction between OA and dynamic light. To do so, we acclimated the bloom-forming SO diatom species *C. debilis* to two pCO_2 concentrations (390 and 1000 µatm) as well as two light regimes (constant and dynamic light), the latter yielding the same integrated irradiance over the day (90 µmol photons m^{-2} s^{-1}). This matrix approach was applied in order to test the hypothesis that dynamic light diminishes the beneficial effect of elevated pCO_2 often observed under constant light, and to understand the physiological mechanisms underlying the general acclimation responses.

Materials and Methods

Culture conditions

Monoclonal cultures of the diatom *Chaetoceros debilis* Cleve 1894 (isolated in 2004 by P. Assmy during R/V Polarstern cruise ANT-XXI/3, European iron fertilization experiment (EIFEX), In-Patch, 49°36′S, 02°05′E; re-isolated by C. Hoppe in 2011) were grown in 1 l glass bottles in semicontinuous dilute-batch cultures (2000–65 000 cells ml^{-1}; diluted every 4–5 d) at 3 ± 0.4°C in a 16 : 8 h, light : dark cycle. Media consisted of 0.2 µm sterile-filtered Antarctic seawater with a salinity of 34 enriched with macronutrients, yielding 180 µmol l^{-1} nitrate, 12 µmol l^{-1} phosphate and 108 µmol l^{-1} silicate. Trace metals and vitamins were added according to F/2 medium (Guillard & Ryther, 1962).

For the constant light treatments (Fig. 1), an irradiance of 90 ± 10 µmol photons m^{-2} s^{-1} was applied. Also for the dynamic light treatments (Fig. 1), an average daily irradiance of 90 ± 10 µmol photons m^{-2} s^{-1} was applied. The dynamic light field was calculated assuming a spring situation with a mixed layer depth of 80 m, a mixing speed of 0.014 m s^{-1} (Denman & Gargett, 1983), five mixing cycles d^{-1} and an attenuation coefficient of 0.04 m^{-1}, leading to a maximum irradiance of 490 µmol photons m^{-2} s^{-1}. The dynamic light modulation (Fig. 1) was controlled via the Control2000 programme of a Rumed incubator (1301; Rubarth Apparate, Laatzen, Germany). In both light treatments, irradiance was provided by identical daylight lamps (Philips Master TL-D 18W; emission peaks at wavelengths of 440, 560 and 635 nm), thus exposing the phytoplankton to the same spectral composition in all treatments. Light intensities were adjusted by neutral density screens and monitored using an LI-1400 data logger (Li-Cor, Lincoln, NE, USA) equipped with a 4π sensor (Walz, Effeltrich, Germany).

Different pCO_2 conditions were achieved by continuous and gentle aeration of the incubation bottles with air of different CO_2 partial pressures (390 and 1000 µatm; gas flow rates *c.* 90 ± 10 ml min^{-1}) delivered through sterile 0.2 µm air filters (Midisart 2000; Sartorius Stedim, Göttingen, Germany). Gas mixtures were generated using a gas flow controller (CGM 2000; MCZ Umwelttechnik, Bad Nauheim, Germany), in which CO_2-free air (< 1 ppmv CO_2; Dominick Hunter, Kaarst, Germany) was mixed with pure CO_2 (Air Liquide Deutschland, Düsseldorf, Germany). The CO_2 concentration in the mixed gas was regularly monitored with a nondispersive infrared analyzer system (LI6252; Li-Cor Biosciences) calibrated with CO_2-free air and purchased gas mixtures of 150 ± 10 and 1000 ± 20 ppmv CO_2 (Air Liquide Deutschland). Cultures were acclimated to treatment conditions for at least 10 generations before sampling, never exceeding 65 000 cells ml^{-1} during this time period.

Continuous aeration with air at the desired CO_2 partial pressure (390 and 1000 µatm) as well as regular dilution of cultures with pre-aerated seawater medium led to stable carbonate chemistry over the course of the experiment (Table 1) and to significant differences between pCO_2 (ANOVA, $P < 0.001$ for dissolved inorganic carbon (DIC), pH and pCO_2), but not between light treatments (ANOVA, $P > 0.05$). In the ambient treatments, pCO_2 concentrations were 382 ± 18 µatm for constant light and 400 ± 17 µatm for dynamic light. In the OA treatments, pCO_2 concentrations were 987 ± 28 µatm for constant light and 1026 ± 31 µatm for dynamic light. Over the duration of the experiment (> 5 wk), the drifts in DIC and TA compared with abiotic controls were < 2% and < 4%, respectively.

Carbonate chemistry

Samples for total alkalinity (TA; $n = 14$) were 0.7 µm filtered (glass fibre filters, GF/F; Whatman, Maidstone, UK) and stored in borosilicate bottles at 3°C. TA was estimated from duplicate potentiometric titration (Brewer *et al.*, 1986) using a TitroLine alpha plus (Schott Instruments, Mainz, Germany) and corrected for systematic errors based on measurements of certified reference materials (CRMs provided by Prof. A. Dickson, Scripps, USA; batch no. 111; reproducibility ± 5 µmol kg^{-1}). DIC ($n = 14$) samples were filtered through 0.2 µm cellulose-acetate filters (Sartorius stedim) and stored in gas-tight borosilicate bottles at 3°C. DIC was measured colorimetrically in triplicates with a QuAAtro autoanalyser (Seal Analytical, Norderstedt, Germany; Stoll *et al.*, 2001). The analyser was calibrated with $NaHCO_3$ solutions (with a salinity of 35, achieved by addition of NaCl) to achieve concentrations ranging from 1800 to 2300 µmol DIC kg^{-1}. CRMs were used for corrections of errors in instrument performance such as baseline drifts (reproducibility ± 8 µmol kg^{-1}). Seawater pH_{total} ($n = 14$) was measured potentiometrically with a two-point calibrated glass reference electrode (IOline; Schott Instruments). An internal TRIS-based reference standard (Dickson *et al.*, 2007) was used to correct for variability in electrode performance (reproducibility ± 0.015 pH units). Following suggestions by Hoppe *et al.* (2012), seawater carbonate chemistry (including pCO_2) was calculated from TA and pH using CO_{2SYS} (Pierrot *et al.*, 2006). The dissociation constants of carbonic acid of Mehrbach *et al.* (1973; refitted by Dickson & Millero, 1987) were used for the calculations. Dissociation constants for $KHSO_4$ were taken from Dickson (1990).

Growth, elemental composition and production rates

Samples for cell counts were fixed with Lugols solution (1% final concentration) and counted on a light microscope (Axio Observer.D1; Zeiss) after 24 h sedimentation time in 10 ml Utermöhl chambers (Hydro-Bios, Kiel, Germany, > 1700 cells counted per sample). Samples for determination of Chl*a* were filtered onto 0.6 µm glass-fibre filters (GF/F; Whatman), immediately placed into liquid nitrogen and stored at −80°C until analysis. Chl was subsequently extracted in 8 ml 90% acetone (2–3 h at 4°C). After removal of the filter, concentrations were determined on a fluorometer (TD-700; Turner Designs, Sunnyvale, CA, USA), using an acidification step (1 M HCl) to determine phaeopigments (Knap *et al.*, 1996). Growth rate determinations started 1–2 d after redilution from daily Chl sampling ($n = 3$) over 4 d (consecutive) within the first 15 min of the dark phase and were calculated as

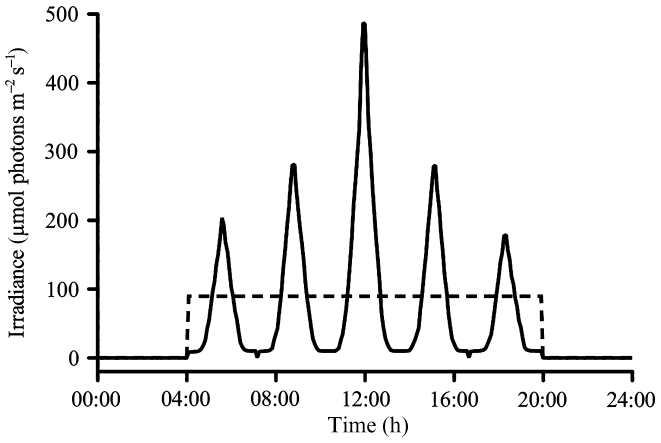

Fig. 1 Applied irradiances (µmol photons m^{-2} s^{-1}) over the day (16 : 8 h, light : dark cycle) in the constant (dashed line) and dynamic (solid line) light regimes.

Table 1 Seawater carbonate chemistry was sampled regularly over the course of the experiments ($n = 14$; mean ± 1 SD)

Treatment	DIC (µmol kg^{-1})	TA (µmol kg^{-1})	pH_{total}	pCO_2 (µatm)
Constant light				
390 µatm CO_2	2092 ± 15	2250 ± 27	8.05 ± 0.02	382 ± 18
1000 µatm CO_2	2202 ± 29	2258 ± 18	7.66 ± 0.03	987 ± 28
Dynamic light				
390 µatm CO_2	2101 ± 27	2263 ± 33	8.03 ± 0.02	400 ± 17
1000 µatm CO_2	2203 ± 25	2252 ± 27	7.65 ± 0.02	1026 ± 31

DIC, dissolved inorganic carbon. CO_2 partial pressure (pCO_2) was calculated from total alkalinity (TA) and pH_{total} at 3°C and a salinity of 34 using CO_2SYS (Pierrot *et al.*, 2006), and concentrations of 12 and 108 µmol kg^{-1} for phosphate and silicate, respectively.

$$\mu = (\log_e[\mathrm{Chl}]_{t2} - \log_e[\mathrm{Chl}]_{t1})/\Delta t \quad \text{Eqn 1}$$

where $[\mathrm{Chl}]_{t1}$ and $[\mathrm{Chl}]_{t2}$ denote the Chl concentrations at the sampling days t_1 and t_2, respectively, and Δt is the corresponding incubation time in d.

Particulate organic carbon (POC) and nitrogen (PON) were measured after filtration onto precombusted (15 h, 500°C) glass-fibre filters (GF/F 0.6 µm nominal pore size; Whatman). Filters were stored at −20°C and dried for at least 12 h at 60°C before sample preparation. Analysis was performed using a CHNS-O elemental analyser (Euro EA 3000; HEKAtech). Contents of POC and PON were corrected for blank measurements and normalized to filtered volume and cell densities to yield cellular quotas. Biogenic silica (BSi) was determined spectrophotometrically after treatment with a molybdate solution as described in Koroleff (1983). Production rates of Chl, POC, PON and BSi were calculated by multiplying the cellular quota with the growth rate of the respective culture. In order to diminish possible short-term effects arising from changes in irradiance fields in the dynamic treatments, all samples were taken within the first 30 min of the dark phase.

Chl-specific net primary production

Chl-specific net primary production (NPP) rates were determined in triplicate by incubation of 20 ml of culture with 20 µCi $NaH^{14}CO_3$ spike (53.1 mCi mmol^{-1}; Perkin Elmer, Waltham, MA, USA) in 20 ml glass scintillation vials for 24 h under experimental conditions. From these incubations, 0.1 ml aliquots were immediately removed, mixed with 15 ml of scintillation cocktail (Ultima Gold AB; PerkinElmer) and counted after 2 h with a liquid scintillation counter (Tri-Carb 2900TR; PerkinElmer) to determine the total amount of added $NaH^{14}CO_3$ ($DPM_{100\%}$). For blank determination ($DPM_{0\%}$), one replicate was immediately acidified with 0.5 ml of 6 M HCl. After 24 h of incubation, ^{14}C incorporation was stopped by adding 0.5 ml of 6 M HCl to each vial. The entire sample was then left to degas and dry in a custom-built chamber. When samples were completely dry (1–2 d), 5 ml milli-Q water were added to resuspend the sample. Subsequently, 15 ml of scintillation cocktail (Ultima Gold AB; PerkinElmer) were added and samples were measured after 2 h with a liquid scintillation counter (Tri-Carb 2900TR; PerkinElmer). NPP rates (µg C (µg Chl)$^{-1}$ d^{-1}) were calculated as

$$\mathrm{NPP} = ([\mathrm{DIC}] \times (\mathrm{DPM_{sample}} - \mathrm{DPM_{0\%}}) \times 1.05))/(\mathrm{DPM_{100\%}} \times t \times [\mathrm{Chl}]) \quad \text{Eqn 2}$$

where [DIC] and [Chl] denote the concentrations of DIC and Chl in the sample, respectively. DPM_{sample} denotes the disintegrations min^{-1} (DPM) in the samples, $DPM_{0\%}$ reflects the blank value, $DPM_{100\%}$ denotes the DPM of the total amount of $NaH^{14}CO_3$ added to the samples, and t is the duration of the incubation.

Variable Chl fluorescence

Photophysiological characteristics, based on photosystem II (PSII) variable Chl fluorescence, were measured using a fast repetition rate fluorometer (FRRf, FastOcean PTX; Chelsea Technologies, West Molesey, UK) in combination with a FastAct Laboratory system (Chelsea Technologies). The excitation wavelength of the fluorometer's light-emitting diodes (LEDs) was 450 nm, and the applied light intensity was 1.3×10^{22} photons m^{-2} s^{-1}. The FRRf was used in single turnover mode, with a saturation phase comprising 100 flashlets on a 2 µs pitch and a relaxation phase comprising 40 flashlets on a 50 µs pitch. All measurements ($n = 3$) were conducted in a temperature-controlled chamber at 3 ± 0.3°C.

The minimum (F_0) and maximum Chl fluorescences (F_m) were estimated from iterative algorithms for induction (Kolber *et al.*, 1998) and relaxation phase (Oxborough, 2012) after subtraction of a blank value (average of $n = 8$ measurements) in the middle of the dark phase (i.e. 4 h after offset of light). Maximum quantum yields of PSII (apparent PSII photochemical quantum efficiency; F_v/F_m) were calculated as

$$F_v/F_m = (F_m - F_0)/F_m \quad \text{Eqn 3}$$

Photosystem II electron flux was calculated on a volume basis (JV_{PSII}; (mol e$^-$ m^{-3} d^{-1})) using the absorption algorithm (Oxborough *et al.*, 2012). The JV_{PSII} rates were converted to Chl-specific absolute rates (ETR (mol e$^-$ (mol Chl)$^{-1}$s^{-1})) by dividing it by the Chl concentration of the sample at the time point of the measurement and the number of seconds per day. Chl-specific JV_{PSII}-based photosynthesis–irradiance (PI) curves were conducted four times a day (1 and 8 h after the onset of light as well as directly after and 4 h after the onset of darkness) at 15 irradiance (I) intensities between 6 and 650 µmol photons m^{-2} s^{-1}, with an acclimation time of 90 s per light step. Following the suggestion by Silsbe & Kromkamp (2012), the light-use efficiency (α), and the light saturation index (I_K) were estimated by fitting the data to the model by Webb *et al.* (1974):

$$\mathrm{ETR} = \alpha \times I_K \times [1 - e^{(-I \times I_K)}] \quad \text{Eqn 4}$$

The maximum electron transport rates (ETR_{max} (mol e$^-$ mol^{-1} Chl s^{-1}) were estimated after applying a beta phase fit as described by Oxborough (2012). Daily electron transport rates ($ETR_{24\,h}$ (mol e$^-$ (mol Chl)$^{-1}$d^{-1})) were estimated by integrating the number of electrons transported over the 16 h light phase. $ETR_{24\,h}$ were calculated in 5 min steps of I-values of both light regimes (i.e. 90 µmol photons m^{-2} s^{-1} under constant and variable irradiances under dynamic light) using α, I_K and ETR_{max} from the PI curve measured closest to the time point of interest. Chl concentrations for normalizations were corrected using the growth rate and the time difference between FRRf and Chl measurements. To estimate the energy transfer efficiency from photochemistry to biomass build-up, the electron requirement for carbon fixation ($\Phi_{e,C}$ (mol e$^-$ (mol C)$^{-1}$)) was calculated for each

treatment by dividing the $ETR_{24\,h}$ by NPP (expressed as molar quantities). It should be noted that differences in the spectral composition of the light used for ETR (i.e. blue light) and NPP measurements (i.e. white light) could lead to a systematic overestimation of $\Phi_{e,C}$.

Nonphotochemical quenching of Chl fluorescence (NPQ) at irradiances of 490 and 650 μmol photons $m^{-2}\,s^{-1}$ (i.e. the maximum irradiance applied in the dynamic light cycle as well as the maximum irradiance step of the PI curve) were calculated using the normalized Stern–Volmer coefficient (also termed NSV) as described in Oxborough (2012) and McKew *et al.* (2013):

$$(F'_q/F'_v) - 1 = F'_0/F'_v \qquad \text{Eqn 5}$$

where F'_0 was measured after each light step (with a duration of 90 s).

Statistics

All data are given as the means of the replicates ± 1 SD. To test for significant differences between the treatments, two-way ANOVAs with additional normality (Shapiro–Wilk) and *post hoc* (Holm–Sidak method) tests were performed. The significance level was set to 0.05. Statistical analyses were performed using the program SigmaPlot (SysStat Software Inc., San Jose, CA, USA).

Results

Growth rates and elemental composition

Chl-specific growth rates (Fig. 2a; Table 2) under constant light conditions were similarly high, being 0.53 ± 0.03 and 0.56 ± 0.03 d^{-1} in ambient and high pCO_2 treatments, respectively. Under dynamic light, growth rates were significantly lower than under constant light (ANOVA, $F = 51$; $P < 0.001$; Table S1). Also under these conditions, growth rates were unaffected by the applied pCO_2 treatments, being 0.44 ± 0.01 d^{-1} at ambient pCO_2 and 0.42 ± 0.03 d^{-1} at high pCO_2.

With respect to the amount of Chl per cell (Table 2), we observed significant effects of both pCO_2 (ANOVA, $F = 28$; $P < 0.001$) and light treatments (ANOVA, $F = 6$; $P = 0.047$). Under dynamic light, Chl quotas significantly decreased with increasing pCO_2 (*post hoc*, $P < 0.001$), while they remained unaffected by OA under constant light, leading to a significant interactive effect of pCO_2 and light intensity on cellular Chl quotas (ANOVA, $F = 21$; $P = 0.002$). Similarly, the production of Chl per cell (Fig. 2b; Table 2) was also significantly affected by both pCO_2 (ANOVA, $F = 18$; $P = 0.003$) and light (ANOVA, $F = 56$; $P < 0.001$). Both factors also had an interactive effect on production rates (ANOVA, $F = 25$; $P = 0.001$), which led to a significant decrease in Chl production under dynamic light and increasing pCO_2 (*post hoc*, $P < 0.001$). The ratio of Chl : C (Table 2) was not significantly affected by any treatment.

Cellular quotas of POC (Table 2) under constant light did not differ between ambient and high pCO_2, whereas they significantly decreased with increasing pCO_2 under dynamic light (*post hoc* test, $P = 0.010$; significant ANOVA interaction between pCO_2 and light, $F = 9$; $P = 0.018$). Overall, POC production (Fig. 2c, Table 2) under constant light was not significantly affected by pCO_2, but was significantly reduced under dynamic vs constant light (ANOVA, $F = 31$; $P < 0.001$). Under dynamic light conditions, POC production also significantly decreased with increasing pCO_2 (*post hoc*, $P = 0.009$), resulting in a significant interaction term between pCO_2 and light conditions (ANOVA, $F = 9$; $P = 0.018$).

Cellular quotas of PON (Table 2) were significantly reduced under high vs ambient pCO_2 (ANOVA, $F = 14$; $P = 0.006$), irrespective of the light conditions applied. Also the production of PON (Fig. 2d; Table 2) decreased significantly with decreasing pCO_2 (ANOVA, $F = 11$; $P = 0.010$). PON production was significantly higher under constant than under dynamic light (ANOVA, $F = 23$; $P = 0.001$). Under constant light, C : N ratios significantly increased with increasing pCO_2 (Fig. 2f; Table 2; *post hoc*, $P = 0.017$). Under dynamic light, no such response was observed. Significant differences in C : N ratios between the light treatments were observed under high pCO_2 only, where dynamic light led to an decrease in C : N (*post hoc*, $P = 0.033$).

Cultures exhibited a highly significant decline in the cellular quota of biogenic silica (BSi; Table 2) with increasing pCO_2 (ANOVA, $F = 38$; $P < 0.001$). BSi quotas were furthermore lower under dynamic than under constant light (ANOVA, $F = 9$; $P = 0.020$). We also observed a highly significant decrease in BSi production (Fig. 2e; Table 2) with increasing pCO_2 (ANOVA, $F = 38$; $P < 0.001$). Furthermore, BSi production was significantly lower under dynamic than under constant light (ANOVA, $F = 90$; $P < 0.001$).

Chl-specific NPP

Chl-specific NPP (Fig. 3; Table 3) under constant light increased slightly, yet insignificantly, with increasing pCO_2. Under dynamic light, NPP was lower than under constant light (ANOVA, $F = 27$; $P < 0.001$; Table S2). Under these conditions, NPP was also significantly decreased with increasing pCO_2 (*post hoc*, $P < 0.001$), resulting in a significant interaction between pCO_2 and light conditions (ANOVA, $F = 7$; $P = 0.028$).

Chl fluorescence-based photophysiology

The dark-acclimated quantum yield efficiency of PSII (F_v/F_m) was similar in all treatments, with values of 0.53 ± 0.01. Neither nonphotochemical quenching (NPQ) at 490 μmol photons $m^{-2}\,s^{-1}$ nor maximal NPQ at 650 μmol photons $m^{-2}\,s^{-1}$ (NPQ_{max}, Table 3) was significantly affected by the applied treatments (Supporting Information, Fig. S1).

The fitted parameters of night-time FRRf-based PI curves (Fig. 4) were strongly influenced by experimental treatments. The maximal electron transport rates through PSII (ETR_{max}; Table 3) increased with increasing pCO_2 (ANOVA, $F = 17$; $P = 0.003$) and were also significantly higher under dynamic than under constant light (ANOVA, $F = 71$; $P < 0.001$). *Post hoc* tests

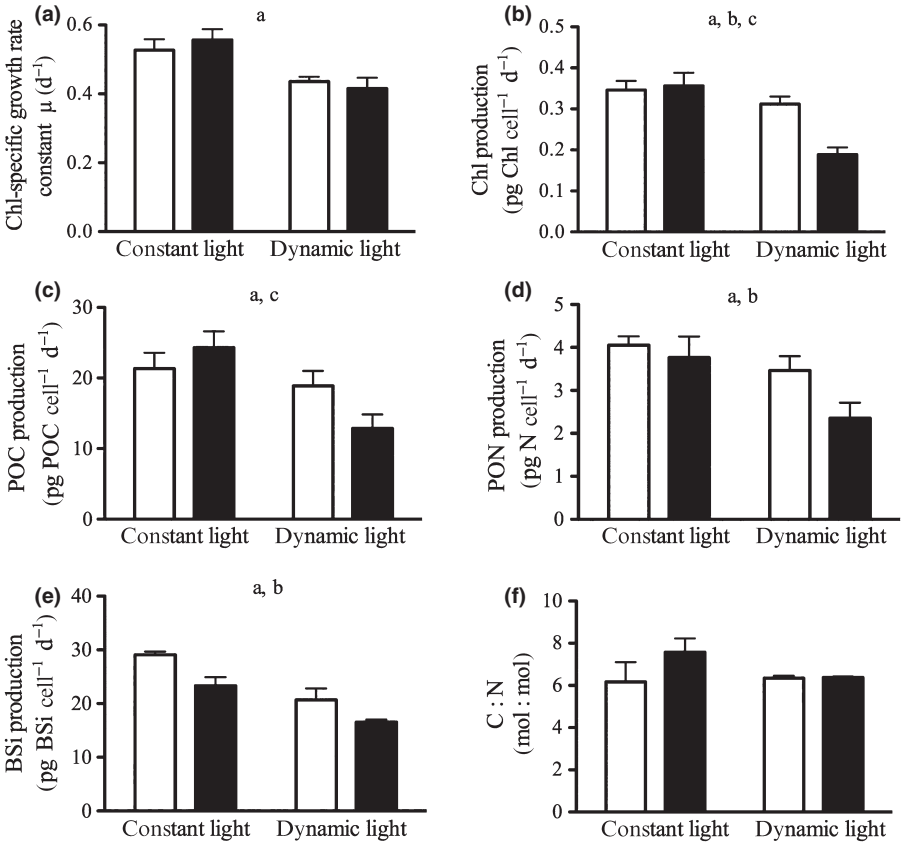

Fig. 2 Chlorophyll-specific growth rate constants (a), production rates of Chl (b), particulate organic carbon (POC) (c), particulate organic nitrogen (PON) (d), BSi (e) and cellular C : N ratios (f) of *Chaetoceros debilis* at pCO_2 concentrations of 390 μatm (open bars) and 1000 μatm (closed bars) under constant and dynamic light regimes ($n = 3$; mean ± 1 SD). Letters indicate significant ($P < 0.05$) differences between: a, light treatments; b, pCO_2 treatments; c, significant interactions between light and pCO_2 treatments.

Table 2 Chlorophyll-specific growth rates, cellular quotas and production rates of Chl, particulate organic carbon (POC), particulate organic nitrogen (PON) and biogenic silica (BSi) of *Chaetoceros debilis* ($n = 3$; mean ± 1 SD) under two pCO_2 concentrations at constant and dynamic light regimes

		Constant light		Dynamic light		
Parameter	Unit	390 μatm CO_2	1000 μatm CO_2	390 μatm CO_2	1000 μatm CO_2	
Chl-specific growth rate	μ (d^{-1})	0.53 ± 0.03	0.56 ± 0.03	0.44 ± 0.01	0.42 ± 0.03	*
Cellular quota	Chl (pg $cell^{-1}$)	0.66 ± 0.04	0.62 ± 0.06	0.72 ± 0.04	0.45 ± 0.04	*,†
	POC (pg $cell^{-1}$)	40.49 ± 4.29	43.66 ± 4.13	43.28 ± 4.91	30.91 ± 4.72	†
	PON (pg $cell^{-1}$)	7.69 ± 0.39	6.76 ± 0.89	7.94 ± 0.77	5.65 ± 0.87	
	BSi (pg $cell^{-1}$)	55.2 ± 1.15	41.87 ± 2.89	47.43 ± 4.88	39.75 ± 1.13	*
Production rates	Chl (pg $cell^{-1}$ d^{-1})	0.35 ± 0.02	0.36 ± 0.03	0.31 ± 0.02	0.19 ± 0.02	*,†
	POC (pg $cell^{-1}$ d^{-1})	21.34 ± 2.26	24.32 ± 2.30	18.88 ± 2.14	12.87 ± 1.96	†
	PON (pg $cell^{-1}$ d^{-1})	4.05 ± 0.21	3.76 ± 0.50	3.47 ± 0.34	2.35 ± 0.36	*
	BSi (pg $cell^{-1}$ d^{-1})	29.09 ± 0.61	23.32 ± 1.61	20.69 ± 2.13	16.55 ± 0.47	*
Elemental ratios	C : N	6.17 ± 0.93	7.58 ± 0.65	6.35 ± 0.12	6.38 ± 0.04	
	Chl : C	61.67 ± 4.70	68.51 ± 5.01	60.44 ± 5.72	67.87 ± 6.56	

Sparkline boxes indicate ocean acidification responses of the measured parameters under the respective light regime. Significant light effects are indicated by asterisks (*), and interactive effects by dagger symbols (†).

revealed that the OA response was much more pronounced under dynamic light (*post hoc*, $P = 0.022$) than under constant light (*post hoc*, $P = 0.222$). No sign of photoinhibition of ETR was observed (Fig. 4). The maximum PSII light-use efficiency (α; Table 3) was significantly higher under OA than under ambient pCO_2 (ANOVA, $F = 14$, $P = 0.006$), a result that was mainly driven by the responses under dynamic light (*post hoc*, $P < 0.001$) and not that pronounced under constant light (*post hoc*, $P = 0.120$). In addition, α-values in both pCO_2 treatments were significantly higher under dynamic than under constant light (ANOVA, $F = 35$; $P < 0.001$). The PSII light saturation point (I_K; Table 3) was not significantly affected by the experimental treatments.

Similarly, cumulative electron transport rates over 24 h ($ETR_{24\,h}$; Table 3) were also higher under OA than under ambient pCO_2 (ANOVA, $F = 9$; $P = 0.029$) as well as under dynamic vs constant light (ANOVA, $F = 7$; $P = 0.015$). The strongest responses were observed under high pCO_2 (*post hoc*, $P = 0.013$)

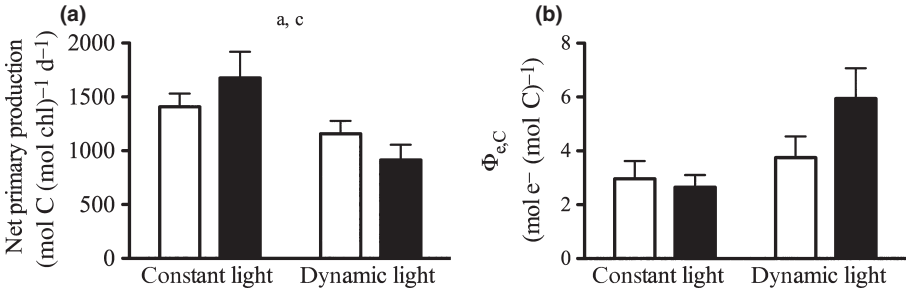

Fig. 3 Chlorophyll-specific net primary production (NPP; a) and electron requirement for carbon fixation ($\Phi_{e,C}$; b) at pCO_2 concentrations of 390 μatm (open bars) and 1000 μatm (closed bars) under constant and dynamic light regimes ($n = 3$; mean ± 1 SD). Letters indicate significant ($P < 0.05$) differences between: a, light treatments; b, pCO_2 treatments; c, significant interactions between light and pCO_2 treatments.

Table 3 Fast repetition rate (FRR)-flourometrical photosystem II (PSII) photochemistry measurements – nonphotochemical quenching at 490 μmol photons m^{-2} s^{-1} (NPQ_{490}), maximal NPQ (NPQ_{max}), maximal absolute electron transfer rates through PSII (ETR_{max}), light saturation index (I_K) and the maximum light-use efficiency (initial slope α) at night (4 h after the onset of darkness) as well as integrated daily ETR ($ETR_{24\,h}$), net primary production (NPP) and energy transfer efficiency from photochemistry to biomass production ($\Phi_{e,C}$) under two pCO_2 concentrations at constant and dynamic light regimes ($n = 3$; mean ± 1 SD)

		Constant light			Dynamic light			
Parameter	Unit	390 μatm CO_2		1000 μatm CO_2	390 μatm CO_2		1000 μatm CO_2	
NPQ_{490}	Dimensionless	1.18 ± 0.31		1.09 ± 0.10	0.86 ± 0.27		0.78 ± 0.15	
NPQ_{max}	Dimensionless	1.64 ± 0.24		1.80 ± 0.19	1.62 ± 0.29		1.60 ± 0.25	
ETR_{max}	mol e$^-$ (mol Chl)$^{-1}$ min^{-1}	8.31 ± 1.37		9.44 ± 0.95	12.04 ± 0.96		15.93 ± 0.86	*
I_K	μmol photons m^{-2} s^{-1}	138 ± 24		130 ± 17	142 ± 9		144 ± 5	
α	mol e$^-$ m^2 (mol Chl)$^{-1}$ (mol photons)$^{-1}$	0.06 ± 0.01		0.07 ± 0.01	0.09 ± 0.01		0.11 ± 0.01	*
$ETR_{24\,h}$	mol e$^-$ (mol Chl)$^{-1}$ d^{-1}	4168 ± 563		4435 ± 108	4346 ± 468		5430 ± 189	*
NPP	mol C (mol Chl)$^{-1}$ d^{-1}	1407 ± 124		1676 ± 243	1158 ± 119		914 ± 142	*,†
$\Phi_{e,C}$	mol e$^-$ (mol C)$^{-1}$	3.00 ± 0.68		2.68 ± 0.33	3.79 ± 0.70		6.04 ± 0.99	*,†

Sparkline boxes indicate ocean acidification responses of the measured parameters under the respective light regime. Significant light effects are indicated by asterisks (*), and interactive effects by dagger symbols (†).

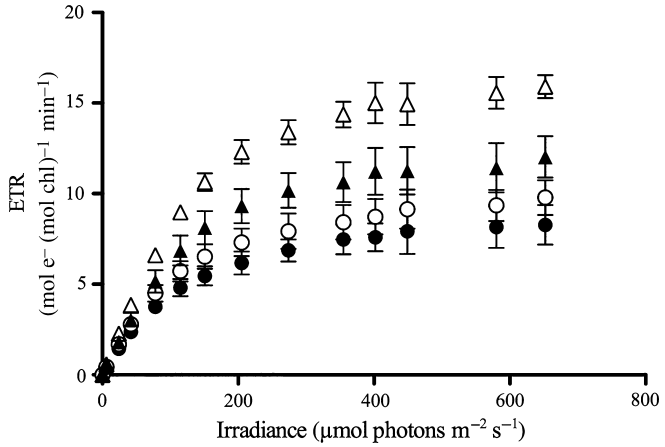

Fig. 4 Night-time responses in Chl-specific electron transport rate (ETR) to increasing irradiance from constant (closed circles) and dynamic light treatments (closed triangles) at 390 μatm pCO_2 as well as from constant (open circles) and dynamic light treatments (open triangles) at 1000 μatm pCO_2 ($n = 3$; mean ± 1 SD).

and dynamic light (*post hoc*, $P = 0.008$). The electron requirement for carbon fixation ($\Phi_{e,C}$; Fig. 3; Table 3) was significantly higher under dynamic than under constant light (ANOVA, $F = 28$; $P < 0.001$). In the dynamic light treatments, $\Phi_{e,C}$ was also much higher under OA compared with ambient pCO_2 (*post hoc*, $P < 0.001$). Such an OA response was not observed under constant light conditions, where $\Phi_{e,C}$ decreased slightly (*post hoc*, $P = 0.047$). Overall, these responses led to a significant effect of pCO_2 (ANOVA, $F = 6$; $P < 0.035$) as well as – because of the opposing OA trends under the two light treatments – a significant interaction term between light treatments and pCO_2 concentrations (ANOVA, $F = 10$; $P < 0.012$).

Discussion

Dynamic light exerts high metabolic costs

Prevailing strong winds lead to deeply mixed surface layers and highly dynamic light regimes in the SO (Nelson & Smith, 1991). Phytoplankton species occurring in this environment can therefore be expected to cope well with dynamic light conditions. In fact, cellular POC and PON quotas as well as C : N and Chl : C at 390 μatm pCO_2 did not differ between the light treatments in *C. debilis* (Table 2). The maintenance of cellular stoichiometry under dynamic light was, however, achieved at the expense of growth and biomass build-up (Figs 2, 3; Table 2). A decline in growth rates under dynamic light is an overarching pattern observed in several studies (van de Poll *et al.*, 2007; Mills *et al.*, 2010; Boelen *et al.*, 2011; Shatwell *et al.*, 2012). Moreover, in the current study, Chl fluorescence-based estimates of the light-use efficiency α and ETR_{max}, as well as daily integrated $ETR_{24\,h}$, were

significantly higher under dynamic than under constant light (Table 3), while NPP and biomass build-up under dynamic light were significantly lowered (Figs 2, 3). This implies that under dynamic light, the overall energy transfer efficiency from photochemistry to net biomass production was substantially reduced (Wagner *et al.*, 2006; Ihnken *et al.*, 2011; Su *et al.*, 2012; Jin *et al.*, 2013).

The electron requirement of carbon fixation ($\Phi_{e,C}$) was indeed significantly higher under dynamic light conditions (Fig. 3), hinting at an increase in other electron-consuming processes such as mitochondrial respiration, photorespiration or alternative electron cycling (Prásil *et al.*, 1996; Badger *et al.*, 2000; Wagner *et al.*, 2006; Waring *et al.*, 2010; Thamatrakoln *et al.*, 2013). While $\Phi_{e,C}$ should theoretically be 4–6 mol e^- (mol C)$^{-1}$ (Genty *et al.*, 1989; Suggett *et al.*, 2009), the estimates for $\Phi_{e,C}$ in this study range between *c.* 3 and 6 mol e^- (mol C)$^{-1}$ (Table 3). Values between 1.2 and 54.3 mol e^- (mol C)$^{-1}$ have been previously observed in field studies and laboratory experiments (Suggett *et al.*, 2009; Lawrenz *et al.*, 2013). Values of $\Phi_{e,C} < 4$ mol e^- (mol C)$^{-1}$ have been attributed to systematic errors in the ETR calculations (Lawrenz *et al.*, 2013). In addition, differences in temporal scales between measures (e.g. Kromkamp & Forster, 2003) as well as short acclimation times may lead to a systematic underestimation of ETRs. Regarding the latter, directional errors in $\Phi_{e,C}$ are, however, unlikely to have contributed to the differences between light regimes, as the treatment-specific variations in α, I_K and ETR_{max} were similar at different time points (data not shown). Irrespective of a potential underestimation of $\Phi_{e,C}$, the observed trends indicate comparably low energy transfer efficiency under dynamic light, which could well explain the observed decrease in growth and NPP compared with constant light (Fig. 3). This interpretation is further corroborated by the observed I_K-independent behaviour of the PI curves (i.e. changes in ETR_{max} and α while I_K stays constant; Table 3), which can be attributed to changes in processes that decouple carbon fixation from photosynthetic electron transport through the consumption of ATP and reductants (Behrenfeld *et al.*, 2004, 2008).

Diatom cells growing under dynamic light need to adjust their photosynthetic apparatus to achieve a balance between photoprotection at high light and effective light-harvesting at low light. No high-light stress was observed in ETR vs irradiance curves (Fig. 4), indicating successful photoprotection under all tested scenarios. In line with other studies on dynamic light (van de Poll *et al.*, 2007; Kropuenske *et al.*, 2009; Alderkamp *et al.*, 2012; Su *et al.*, 2012), we also did not observe an increase in NPQ capacity (Table 3). Successful photoprotection may be achieved via other processes such as increased connectivity between reaction centres (Trimborn *et al.*, 2014) or the induction of alternative electron pathways (e.g. Mehler reaction, electron flow around PSII or PSI) that can supplement the xanthophyll cycle in diatoms (Prásil *et al.*, 1996; Asada, 1999; Waring *et al.*, 2010). These mechanisms could have contributed to the observed increase in $\Phi_{e,C}$ (Fig. 3) under dynamic vs constant light.

In addition, the apparent insensitivity of electron transport towards high-light stress (Fig. 4) does not mean that no photodamage of reaction centres occurs. In fact, an uncoupling between PSII inactivation and the rate of electron flow has been described as a common mechanism for phytoplankton under natural light regimes (Behrenfeld *et al.*, 1998). The uncoupling can be explained by the presence of 'excess PSII capacity' (i.e. more reaction centres than are actually needed), allowing for high photochemical efficiencies even if light-dependent photoinactivation of PSII increases (Behrenfeld *et al.*, 1998). This overproduction and subsequent repair of PSII, including the susceptible D1 subunit and associated proteins, imposes high metabolic costs for the phytoplankton cell (Raven, 2011). Whether or not the costs, being associated with the high-light phases of the dynamic light treatment, are compensated for by the subsequent period of low light depends on the rates of both, the changes in light intensity and D1 repair (Behrenfeld *et al.*, 1998; Marshall *et al.*, 2000). In the tested scenarios here, we did not observe the manifestation of photoinhibition (Fig. 4). Therefore, we postulate that a large fraction of the decline in growth and energy transfer efficiency from photochemistry to biomass production under dynamic light (Fig. 3; Table 3) results from increased metabolic costs of photoprotection and elevated D1 turnover at high light in combination with the consequences of light limitation in the low-light phases.

Ocean acidification increases energy-use efficiency under constant light

Changes in CO_2 supply have been shown to differentially affect SO diatoms on the species level (Boelen *et al.*, 2011; Hoogstraten *et al.*, 2012a,b; Trimborn *et al.*, 2013, 2014) as well as in natural communities (Tortell *et al.*, 2008; Feng *et al.*, 2010; Hoppe *et al.*, 2013). The Antarctic diatom *C. debilis* was shown to exhibit increased energy-use efficiencies (i.e. higher growth rates, but lower O_2 evolution) as well as decreased dark respiration under high pCO_2 and constant light (Trimborn *et al.*, 2013, 2014). In the present study, C : N ratios were higher under OA and constant light, while growth rates and NPP of *C. debilis* were only slightly stimulated under these conditions (Figs 2, 3; Tables 2, 3). The differences in the CO_2 sensitivity of *C. debilis* most likely originate from different pCO_2 treatments applied in the two studies, as significant changes were mainly observed between intermediate (ambient) and low (glacial) pCO_2 concentrations, the latter not being investigated in the current study. Similar to our results, two other species of *Chaetoceros* also showed little or no growth response to OA, but these results apparently also depended on the applied light intensities (Boelen *et al.*, 2011; Ihnken *et al.*, 2011). In CO_2 manipulation experiments with SO phytoplankton communities, however, *Chaetoceros* was found to benefit from elevated pCO_2, as this genus dominated the applied OA treatments (Tortell *et al.*, 2008; Feng *et al.*, 2010).

Such OA responses have often been attributed to the mode of CCMs, which can differ in the ability to reach rate saturation and to respond to environmental changes as well as in the associated costs of these processes. In the case of diatoms, CCMs have been shown to be very effective avoiding carbon limitation, but also to be regulated as a function of external CO_2 concentration (e.g. Raven & Johnston, 1991; Trimborn *et al.*, 2009; Hopkinson *et al.*, 2011). Elevated pCO_2 often leads to a down-regulation

of CCM activity, thereby reducing the overall costs of carbon acquisition (Burkhardt *et al.*, 2001; Rost *et al.*, 2003; Hopkinson *et al.*, 2011). Even though Trimborn *et al.* (2013) observed a rather constitutively expressed CCM for *C. debilis*, it can be speculated that the higher gross CO_2 uptake under elevated pCO_2 may have contributed to the observed stimulation in growth. In conclusion, the often documented beneficial OA effects at constant light could, to a large degree, be explained by overall lowered costs of the CCM.

Photoacclimation can also be influenced by CO_2 via the CO_2-dependent regulation of CCMs and RubisCO concentrations, as these properties can affect the amount of electrons being used during carbon fixation (Tortell, 2000; Rost *et al.*, 2006; Reinfelder, 2011). Trimborn *et al.* (2014) showed strong effects of short-term exposure to low pCO_2 concentrations on various photophysiological parameters in *C. debilis*. In line with findings on two *Thalassiosira* species (McCarthy *et al.*, 2012), ETR_{max} increased with increasing pCO_2 (Table 3), indicating higher substrate saturation at RubisCO and higher activities of the Calvin cycle under OA and constant light. With respect to the balance between light and dark reaction of photosynthesis, we observed a slight decrease in $\Phi_{e,C}$ with increasing pCO_2 (Fig. 3; Table 3). These results could imply that the Calvin cycle acts as a better energy sink under elevated pCO_2 and constant light, as has been proposed by Trimborn *et al.* (2014). Such an increase in electron-use efficiency could thus explain the beneficial effects of OA (Figs 2, 3).

Dynamic light reverses the responses to ocean acidification

In line with previous findings on *Chaetoceros* (Boelen *et al.*, 2011; Ihnken *et al.*, 2011), we observed slight, yet insignificant, enhancement in growth, POC production and NPP with increasing pCO_2 under constant light (Figs 2, 3). In other studies, growth and NPP of *Chaetoceros* were strongly stimulated under elevated pCO_2 (Tortell *et al.*, 2008; Feng *et al.*, 2010; Hoppe *et al.*, 2013; Trimborn *et al.*, 2013). When comparing these trends with the OA responses from the dynamic light treatments, a completely different picture emerges: POC production and NPP decrease under OA by *c.* 30 and 50%, respectively. The putatively beneficial effects of elevated pCO_2 seem not only to be dampened, but even reversed under dynamic light as cells significantly slow down biomass production (Fig. 2). Boelen *et al.* (2011) did not observe any significant responses of *C. brevis* to either OA or dynamic light. Their results indicate a low sensitivity of this strain to increasing pCO_2 up to 750 µatm, even though POC production under OA was reduced by *c.* 15% in their dynamic high-light treatment. In line with our study, Jin *et al.* (2013) observed a decline in carbon fixation rates of the coccolithophore *G. oceanica* under OA and short-term exposure to dynamic light.

Surprisingly, the decline in biomass build-up in this study was observed even though electron transport through PSII was most efficient under these conditions (Table 3). In addition, there was no sign of photoinhibition after short-term exposure to irradiances up to 650 µmol photons m^{-2} s^{-1} in any of the treatments (Fig. 4). At higher irradiances, however, rETRs in *C. debilis* were found to decrease (Trimborn *et al.*, 2014). The photophysiological results therefore suggest that the excess capacity of photosynthesis (Behrenfeld *et al.*, 1998) was sufficient to prevent chronic photoinhibition under the applied assay irradiances (Fig. 4). As these photophysiological results do not explain the decline in POC production and NPP observed under OA and dynamic light (Figs 2, 3) and as the observed I_K-independent changes in the PI curves (Table 3) are indicative of changes in the demand and distribution of energy and reductive equivalents (Behrenfeld *et al.*, 2004, 2008), the underlying reason may be associated with an imbalance between light and dark reactions of photosynthesis.

There is increasing evidence that diatoms are more susceptible to D1 inactivation and photoinhibition under OA than under ambient pCO_2 concentrations (Wu *et al.*, 2010; Gao *et al.*, 2012a; McCarthy *et al.*, 2012). Li & Campbell (2013) observed that under OA, *Thalassiosira pseudonana* has enhanced growth rates under low, but not high light, a finding that is in line with studies on cyanobacteria and coccolithophores (Kranz *et al.*, 2010; Rokitta & Rost, 2012). As photosynthesis shifts progressively from light towards carbon limitation under increasing irradiance, CCM activity also needs to be increased under these conditions (Beardall, 1991; Rost *et al.*, 2006). The CCM, however, is typically down-regulated under OA (Burkhardt *et al.*, 2001; Rost *et al.*, 2003), which could restrict the capacity to rapidly sink more electrons in the Calvin cycle or to drain excess energy by HCO_3^- cycling under short-term high-light stress (Tchernov *et al.*, 1997; Rost *et al.*, 2006). This could result in a lower capability to cope with high light and could increase photoinactivation of PSII under OA (Beardall & Giordano, 2002; Ihnken *et al.*, 2011; Gao *et al.*, 2012b), shifting the susceptibility to photoinhibition towards lower irradiances. The proposed mechanism implies that, under dynamic light, cells exposed to higher pCO_2 concentrations experience high-light stress for longer time periods compared with cells grown under ambient pCO_2. Under constant light, no photoacclimation to high-light phases would be needed, so that an OA-induced surplus of energy could be directly used to build more biomass (Figs 2, 3; Tortell *et al.*, 2008; Trimborn *et al.*, 2013). Under dynamic light, however, this extra energy may lead to higher metabolic costs for photoacclimation and D1 repair during high-light phases, which apparently cannot be compensated by lowered operational costs of CCMs. The mechanism proposed here could collectively explain the observed higher demand for energy and reductive equivalents (i.e. I_K-independent increase in ETR_{max}, Table 3; Behrenfeld *et al.*, 2004), as well as the decline in NPP under OA and dynamic light, ultimately leading to a strong increase in $\Phi_{e,C}$ (Fig. 3).

Under the conditions applied here, *C. debilis* seems to be able to circumvent measurable photoinhibition, even though we speculate that this comes at a high cost, especially under OA combined with dynamic light. Under higher pCO_2 concentrations as well as higher average or more dynamic irradiances, however, OA could induce measurable damage to the photosynthetic apparatus in addition to presumably high metabolic costs incurred from

D1 turnover and photosystem repair (Raven, 2011; Li & Campbell, 2013). Therefore, the modulation of OA responses probably also varies depending on the light regime applied (cf. Boelen *et al.*, 2011). Further, the response pattern may be modulated by depth-dependent changes in the spectral composition of light (Falkowski & LaRoche, 1991), which were not investigated in the present study. In view of the generally high plasticity of photoacclimation in diatoms (Wagner *et al.*, 2006; Lavaud *et al.*, 2007), the interactive effects described here might be even more pronounced in other phytoplankton taxa. In any case, our data have demonstrated that a combination of OA and dynamic light could impose significantly more stress onto phytoplankton than was previously thought.

Implications for ecology and biogeochemistry

In summary, dynamic light was shown to drastically alter OA effects on an ecologically important SO diatom species, leading to a strong decline in primary production under OA and dynamic light. The observed response patterns can be explained by changes in the cellular energetic balance, as the energy transfer efficiency from photochemistry to biomass production was drastically reduced under OA and dynamic light. Given the increasing number of studies dealing with possible interactive effects of OA with high-light stress on phytoplankton (e.g. Wu *et al.*, 2010; Gao *et al.*, 2012a; Gao & Campbell, 2014), the importance of excess PSII capacity should be investigated in future.

Our results also have important implications for the current understanding of OA effects on marine phytoplankton. As has been shown for several environmental variables, such as temperature (e.g. Tatters *et al.*, 2013) or nutrient concentrations (e.g. Fu *et al.*, 2010; Hoppe *et al.*, 2013), interactive effects need to be considered when predicting future productivity and ecosystem functioning. As a central feature of oceanic environments, dynamic light is an especially important aspect (Mitchell *et al.*, 1991; MacIntyre *et al.*, 2000), which has been neglected in most OA studies so far. If our results are representative, the often proposed 'CO_2 fertilization' may be dampened or even reversed in many natural environments. In this context, it is important to consider that anthropogenic CO_2 emissions do not only lead to OA, but also to a warming of the surface ocean (Sarmiento *et al.*, 2004). A concomitant shoaling of the upper mixed layer would thus change the integrated intensity and variability of the light regimes encountered by phytoplankton cells (Rost *et al.*, 2008; Steinacher *et al.*, 2010), making the interactive relationship between OA and light regimes even more important to consider.

Regarding the SO, it seems likely that synergistic effects of iron limitation and dynamic light, both dominant features of this region (Boyd, 2002; de Baar *et al.*, 2005; Alderkamp *et al.*, 2012), jointly lower the potential benefits of OA. Under iron-enriched conditions, as in the present study, diatom taxa such as *Chaetoceros* and *Fragilariopsis* have been shown to dominate OA treatments under constant light, suggesting a higher potential for export production (Tortell *et al.*, 2008; Hoppe *et al.*, 2013). The lowered NPP under OA and dynamic light, however, questions the reliability of such predictions. The aspect of ballasting also has to be considered, as siliceous frustules make diatoms efficient vectors for carbon (Sarthou *et al.*, 2005). In line with Milligan *et al.* (2004), we observed a decline in both cellular BSi quotas and production rates with increasing pCO_2 (Fig. 2; Table 2), which further argues against a stimulation of the biological carbon pump. To date, the effects of dynamic light on OA responses and the underlying reasons for them, as observed in this study, were unknown. This new knowledge will change our perception of phytoplankton under climate change.

Acknowledgements

We would like to thank D. Campbell, N. Schuback and two anonymous reviewers for very helpful comments of this manuscript. We also would like to thank T. Brenneis, J. Hölscher, U. Richter, N. Schuback and S. Beszteri for laboratory assistance. C.J.M.H. and B.R. were funded by the European Research Council (ERC) under the European Community's Seventh Framework Programme (FP7/2007-2013), ERC grant agreement no. 205150. L-M.H. was funded by the German Federal Ministry of Education and Research, project ZeBiCa^2 (31P7279). S.T. was funded by the Helmholtz Impulse Fond (HGF Young Investigator Group EcoTrace).

References

Alderkamp A-C, Kulk G, Buma AGJ, Visser RJW, Van Dijken GL, Mills MM, Arrigo KR. 2012. The effect of iron limitation on the photophysiology of *Phaeocystis antarctica* (Prymnesiophyceae) and *Fragilariopsis cylindrus* (Bacillariophyceae) under dynamic irradiance. *Journal of Phycology* **48**: 45–59.

Asada K. 1999. The water–water cycle in chloroplasts: scavenging of active oxygens and dissipation of excess photons. *Annual Review of Plant Physiology and Plant Molecular Biology* **50**: 601–639.

de Baar H, Boyd P, Coale K, Landry M, Tsuda A. 2005. Synthesis of iron fertilization experiments: from the Iron Age in the Age of Enlightenment. *Journal of Geophysical Research* **110**: C09S16.

Badger MR, Andrews TJ, Whitney SM, Ludwig M, Yellowlees DC, Leggat W, Price GD. 1998. The diversity and coevolution of Rubisco, plastids, pyrenoids, and chloroplast-based CO_2-concentrating mechanisms in algae. *Canadian Journal of Botany-Revue Canadienne De Botanique* **76**: 1052–1071.

Badger MR, von Caemmerer S, Ruuska S, Nakano H. 2000. Electron flow to oxygen in higher plants and algae: rates and control of direct photoreduction (Mehler reaction) and rubisco oxygenase. *Philosophical Transactions of the Royal Society of London. Series B, Biological Sciences* **355**: 1433–1446.

Beardall J. 1991. Effects of photon flux density on the 'CO_2-concentrating mechanism' of the cyanobacterium *Anabaena variabilis*. *Journal of Plankton Research* **13**: 133–141.

Beardall J, Giordano M. 2002. Ecological implications of microalgal and cyanobacterial CO_2 concentrating mechanisms, and their regulation. *Functional Plant Biology* **29**: 335–347.

Behrenfeld MJ, Halsey KH, Milligan AJ. 2008. Evolved physiological responses of phytoplankton to their integrated growth environment. *Philosophical Transactions of the Royal Society* **363**: 2687–2703.

Behrenfeld MJ, Prasil O, Babin M, Bruyant F. 2004. In search of a physiological basis for covariations in light-limited and light-saturated photosynthesis. *Journal of Phycology* **40**: 4–25.

Behrenfeld MJ, Prasil O, Kolber Z, Babin M, Falkowski P. 1998. Compensatory changes in Photosystem II electron turnover rates protect photosynthesis from photoinhibition. *Photosynthesis Research* **58**: 259–268.

Boelen P, van de Poll WH, van der Strate HJ, Neven IA, Beardall J, Buma AGJ. 2011. Neither elevated nor reduced CO_2 affects the photophysiological

performance of the marine Antarctic diatom *Chaetoceros brevis*. *Journal of Experimental Marine Biology and Ecology* **406**: 38–45.

Boyd PW. 2002. Environmental factors controlling phytoplankton processes in the Southern Ocean. *Journal of Phycology* **38**: 844–861.

Brewer PG, Bradshaw AL, Williams RT. 1986. Measurement of total carbon dioxide and alkalinity in the North Atlantic ocean in 1981. In: Trabalka JR, Reichle DE, eds. *The changing carbon cycle – a global analysis*. Heidelberg, Berlin, Germany: Springer Verlag, 358–381.

Burkhardt S, Amoroso G, Riebesell U, Sültemeyer D. 2001. CO_2 and HCO_3^- uptake in marine diatoms acclimated to different CO_2 concentrations. *Limnology and Oceanography* **46**: 1378–1391.

Denman KL, Gargett AE. 1983. Time and space scales of vertical mixing and advection of phytoplankton in the upper ocean. *Limnology and Oceanography* **28**: 801–815.

Dickson AG. 1990. Standard potential of the reaction: $AgCl(s) + ½ H^2(g) = Ag(s) + HCl(aq)$, and the standard acidity constant of the ion HSO_4^- in synthetic seawater from 273.15 to 318.15 K. *Journal of Chemical Thermodynamics* **22**: 113–127.

Dickson AG, Millero FJ. 1987. A comparison of the equilibrium constants for the dissociation of carbonic acid in seawater media. *Deep-Sea Research* **34**: 1733–1743.

Dickson AG, Sabine CL, Christian JR. 2007. *Guide to best practices for ocean CO_2 measurements*. Sidney, BC, Canada: PICES Special Publication 3.

Falkowski PG, LaRoche J. 1991. Acclimation to spectral irradiance in algae. *Journal of Phycology* **27**: 8–14.

Feng Y, Hare CE, Rose JM, Handy SM, DiTullio GR, Lee PA, Smith WO Jr, Peloquin J, Tozzi S, Sun J *et al.* 2010. Interactive effects of iron, irradiance and CO_2 on Ross Sea phytoplankton. *Deep Sea Research Part I: Oceanographic Research Papers* **57**: 368–383.

Fu FX, Place AR, Garcia NS, Hutchins DA. 2010. CO_2 and phosphate availability control the toxicity of the harmful bloom dinoflagellate *Karlodinium veneficum*. *Aquatic Microbial Ecology* **59**: 55–65.

Gao K, Campbell DA. 2014. Photophysiological responses of marine diatoms to elevated CO_2 and decreased pH: a review. *Functional Plant Biology* **41**: 449–459.

Gao K, Helbling EW, Häder D-P, Hutchins DA. 2012b. Responses of marine primary producers to interactions between ocean acidification, solar radiation, and warming. *Marine Ecology Progress Series* **470**: 167–189.

Gao K, Xu J, Gao G, Li Y, Hutchins DA, Huang B, Wang L, Zheng Y, Jin P, Cai X *et al.* 2012a. Rising CO_2 and increased light exposure synergistically reduce marine primary productivity. *Nature Climate Change* **2**: 519–523.

Genty B, Briantais J-M, Baker NR. 1989. The relationship between the quantum yield of photosynthetic electron transport and quenching of chlorophyll fluorescence. *Biochimica et Biophysica Acta* **990**: 87–92.

Guillard RRL, Ryther JH. 1962. Studies of marine planktonic diatoms. I. *Cyclothella nana* Hustedt and *Detonula confervacea* Cleve. *Canadian Journal of Microbiology* **8**: 229–239.

Hoogstraten A, Peters M, Timmermans KR, de Baar HJW. 2012b. Combined effects of inorganic carbon and light on *Phaeocystis globosa* Scherffel (Prymnesiophyceae). *Biogeosciences* **9**: 1885–1896.

Hoogstraten A, Timmermans KR, de Baar HJW. 2012a. Morphological and physiological effects in *Proboscia alata* (Bacillariophyceae) grown under different light and CO_2 concentrations of the modern Southern Ocean. *Journal of Phycology* **48**: 559–568.

Hopkinson BM, Dupont CL, Allen AE, Morel FMM. 2011. Efficiency of the CO_2-concentrating mechanism of diatoms. *Proceedings of the National Academy of Sciences, USA* **108**: 3830–3837.

Hoppe CJM, Hassler CS, Payne CD, Tortell PD, Rost B, Trimborn S. 2013. Iron limitation modulates ocean acidification effects on Southern Ocean phytoplankton communities. *PLoS ONE* **8**: e79890.

Hoppe CJM, Langer G, Rokitta SD, Wolf-Gladrow DA, Rost B. 2012. Implications of observed inconsistencies in carbonate chemistry measurements for ocean acidification studies. *Biogeosciences* **9**: 2401–2405.

Ihnken S, Roberts S, Beardall J. 2011. Differential responses of growth and photosynthesis in the marine diatom *Chaetoceros muelleri* to CO_2 and light availability. *Phycologia* **50**: 182–193.

Jin P, Gao K, Villafañe VE, Campbell DA, Helbling EW. 2013. Ocean acidification alters the photosynthetic responses of a coccolithophorid to fluctuating ultraviolet and visible radiation. *Plant Physiology* **162**: 2084–2094.

Khatiwala S, Primeau F, Hall T. 2009. Reconstruction of the history of anthropogenic CO_2 concentrations in the ocean. *Nature* **462**: 346–349.

Knap A, Michaels A, Close A, Ducklow H, Dickson AD, eds. 1996. Protocols for the Joint Global Ocean Flux Study (JGOFS) core measurements. In: *JGOFS report nr. 19*. Oak Ridge, TN, USA: UNESCO, 170.

Kolber ZS, Prásil O, Falkowski PG. 1998. Measurements of variable chlorophyll fluorescence using fast repetition rate techniques. I. Defining methodology and experimental protocols. *Biochimica et Biophysica Acta* **1367**: 88–106.

Koroleff F. 1983. Determination of silicon. In: Grasshoff K, Kremling K, Ehrhardt M, eds. *Methods of seawater analysis*. Weinheim, Germany: Verlag Chemie, 174–183.

Kranz SA, Levitan O, Richter K-U, Prášil O, Berman-Frank I, Rost B. 2010. Combined effects of CO_2 and light on the N_2-fixing cyanobacterium *Trichodesmium* IMS101: physiological responses. *Plant Physiology* **154**: 334–345.

Kromkamp JC, Forster RM. 2003. The use of variable fluorescence measurements in aquatic ecosystems: differences between multiple and single turnover measuring protocols and suggested terminology. *European Journal of Phycology* **38**: 103–112.

Kropuenske LR, Mills MM, van Dijken GL, Bailey S, Robinson DH, Welschmeyer NA, Arrigo KR. 2009. Photophysiology in two major Southern Ocean phytoplankton taxa: photoprotection in *Phaeocystis antarctica* and *Fragilariopsis cylindrus*. *Limnology and Oceanography* **54**: 1176–1196.

Langer G, Nehrke G, Probert I, Ly J, Ziveri P. 2009. Strain-specific responses of *Emiliania huxleyi* to changing seawater carbonate chemistry. *Biogeosciences* **6**: 2637–2646.

Lavaud J, Strzepek RF, Kroth PG. 2007. Photoprotection capacities differ among plankton diatoms: possible consequence on their spatial distribution related to fluctuations in the underwater light climate. *Limnology and Oceanography* **52**: 1188–1194.

Lawrenz E, Silsbe G, Capuzzo E, Ylöstalo P, Forster RM, Simis SGH, Prášil O, Kromkamp JC, Hickman AE, Moore CM *et al.* 2013. Predicting the electron requirement for carbon fixation in seas and oceans. *PLoS ONE* **8**: e58137.

van Leeuwe MA, van Sikkelerus B, Gieskes WWC, Stefels J. 2005. Taxon-specific differences in photoacclimation to fluctuating irradiance in an Antarctic diatom and a green flagellate. *Marine Ecology Progress Series* **288**: 9–19.

Li G, Campbell DA. 2013. Rising CO_2 interacts with growth light and growth rate to alter photosystem II photoinactivation of the coastal diatom *Thalassiosira pseudonana*. *PLoS ONE* **8**: e55562.

MacIntyre HL, Kana TM, Geider RJ. 2000. The effect of water motion on short-term rates of photosynthesis by marine phytoplankton. *Trends in Plant Science* **5**: 12–17.

Marinov I, Gnanadesikan A, Toggweiler JR, Sarmiento JL. 2006. The Southern Ocean biogeochemical divide. *Nature* **441**: 964–967.

Marshall HL, Geider RJ, Flynn KJ. 2000. A mechanistic model of photoinhibition. *New Phytologist* **145**: 347–359.

Martin JH. 1990. Glacial-interglacial CO_2 change: the Iron Hypothesis. *Paleoceanography* **5**: 1–13.

McCarthy A, Rogers SP, Duffy SJ, Campbell DA. 2012. Elevated carbon dioxide differentially alters the photophysiology of *Thalassiosira pseudonana* (Bacillariophyceae) and *Emiliania huxleyi* (Haptophyta). *Journal of Phycology* **48**: 635–646.

McKew BA, Davey P, Finch SJ, Hopkins J, Lefebvre SC, Metodiev MV, Oxborough K, Raines CA, Lawson T, Geider RJ. 2013. The trade-off between the light-harvesting and photoprotective functions of fucoxanthin-chlorophyll proteins dominates light acclimation in *Emiliania huxleyi* (clone CCMP 1516). *New Phytologist* **200**: 74–85.

Mehrbach C, Culberson CH, Hawley JE, Pytkowicz RM. 1973. Measurement of the apparent dissociation constants of carbonic acid in seawater at atmospheric pressure. *Limnology and Oceanography* **18**: 897–907.

Milligan AJ, Varela DE, Brzezinski MA, Morel FMM. 2004. Dynamics of silicon metabolism and silicon isotopic discrimination in a marine diatom as a function of pCO_2. *Limnology and Oceanography* **49**: 322–329.

Mills MM, Kropuenske LR, van Dijken GL, Alderkamp A-C, Berg GM, Robinson DH, Welschmeyer NA, Arrigo KR. 2010. Photophysiology in two Southern Ocean phytoplankton taxa: photosynthesis of *Phaeocystis antarctica* (Prymnesiophyceae) and *Fragilariopsis cylindrus* (Bacillariopyceae) under simulated mixed-layer irradiance. *Journal of Phycology* **46**: 1114–1127.

Mitchell BG, Brody EA, Holm-Hansen O, McClain C, Bishop J. 1991. Light limitation of phytoplankton biomass and macronutrient utilization in the Southern Ocean. *Limnology and Oceanography* **36**: 1662–1677.

Moore CM, Seeyave S, Hickman AE, Allen JT, Lucas MI, Planquette H, Pollard RT, Poulton AJ. 2007. Iron–light interactions during the Crozet natural iron bloom and export experiment (CrozEx) I: phytoplankton growth and photophysiology. *Deep Sea Research Part II: Topical Studies in Oceanography* **54**: 2045–2065.

Moore JK, Abbott MR, Richman JG, Nelson DM. 2000. The southern ocean at the Last Glacial Maximum: a strong sink for atmospheric carbon dioxide. *Global Biogeochemical Cycles* **14**: 455–475.

Morel FMM, Reinfelder JR, Roberts SB, Chamberlain CP, Lee JG, Yee D. 1994. Zinc and carbon co-limitation of marine phytoplankton. *Nature* **369**: 740–742.

Nelson DM, Smith WOJ. 1991. Sverdrup revisited: critical depths, maximum chlorophyll levels, and the control of Southern Ocean productivity by the irradiance-mixing regime. *Limnology and Oceanography* **36**: 1650–1661.

Nelson DM, Treguer P, Brzezinski MA, Leynaert A, Queguiner B. 1995. Production and dissolution of biogenic silica in the ocean – revised global estimates, comparison with regional data and relationship to biogenic sedimentation. *Global Biogeochemical Cycles* **9**: 359–372.

Oxborough K. 2012. *FastPro8 GUI and FRRf3 systems documentation*. West Molesey, UK: Chelsea Technologies Group Ltd.

Oxborough K, Moore CM, Suggett DJ, Lawson T, Chan HG, Geider RJ. 2012. Direct estimation of functional PSII reaction center concentration and PSII electron flux on a volume basis: a new approach to the analysis of Fast Repetition Rate fluorometry (FRRf) data. *Limnology and Oceanography, Methods* **10**: 142–154.

Pierrot DE, Lewis E, Wallace DWR. 2006. *MS exel program developed for CO_2 system calculations. (ORNL/CDIAC-105a carbon dioxide information analysis centre*. ORNL, TN, USA: US Department of Energy.

van de Poll WH, Visser RJW, Buma AGJ. 2007. Acclimation to a dynamic irradiance regime changes excessive irradiance sensitivity of *Emiliania huxleyi* and *Thalassiosira weissflogii*. *Limnology and Oceanography* **52**: 1430–1438.

Prásil O, Kolber Z, Berry J, Falkowski P. 1996. Cyclic electron flow around Photosystem II *in vivo*. *Photosynthesis Research* **48**: 395–410.

Raven JA. 2011. The cost of photoinhibition. *Physiologia Plantarum* **142**: 87–104.

Raven JA, Johnston AM. 1991. Mechanisms of inorganic-carbon acquisition in marine phytoplankton and their implications for the use of other resources. *Limnology and Oceanography* **36**: 1701–1714.

Reinfelder JR. 2011. Carbon concentrating mechanisms in eukaryotic marine phytoplankton. *Annual Review of Marine Science* **3**: 291–315.

Reinfelder JR, Kraepiel AML, Morel FMM. 2000. Unicellular C_4 photosynthesis in a marine diatom. *Nature* **407**: 996–999.

Rokitta SD, Rost B. 2012. Effects of CO_2 and their modulation by light in the life-cycle stages of the coccolithophore *Emiliania huxleyi*. *Limnology and Oceanography* **57**: 607–618.

Rost B, Riebesell U, Burkhardt S, Sültemeyer D. 2003. Carbon acquisition of bloom-forming marine phytoplankton. *Limnology and Oceanography* **48**: 55–67.

Rost B, Riebesell U, Sültemeyer D. 2006. Carbon acquisition of marine phytoplankton: effect of photoperiod length. *Limnology and Oceanography* **51**: 12–20.

Rost B, Zondervan I, Wolf-Gladrow D. 2008. Sensitivity of phytoplankton to future changes in ocean carbonate chemistry: current knowledge, contradictions and research directions. *Marine Ecology Progress Series* **373**: 227–237.

Sarmiento JL, Slater R, Barber R, Bopp L, Doney SC, Hirst AC, Kleypas J, Matear R, Mikolajewicz U, Monfray P *et al.* 2004. Response of ocean ecosystems to climate warming. *Global Biogeochemical Cycles* **18**: GB3003.

Sarthou G, Timmermans KR, Blain S, Tréguer P. 2005. Growth physiology and fate of diatoms in the ocean: a review. *Journal of Sea Research* **53**: 25–42.

Shatwell T, Nicklisch A, Köhler J. 2012. Temperature and photoperiod effects on phytoplankton growing under simulated mixed layer light fluctuations. *Limnology and Oceanography* **57**: 541–553.

Sigman DM, Hain MP, Haug GH. 2010. The polar ocean and glacial cycles in atmospheric CO_2 concentration. *Nature* **466**: 47–55.

Silsbe GM, Kromkamp JC. 2012. Modeling the irradiance dependency of the quantum efficiency of photosynthesis. *Limnology and Oceanography, Methods* **10**: 645–652.

Steinacher M, Joos F, Frölicher TL, Bopp L, Cadule P, Cocco V, Doney SC, Gehlen M, Lindsay K, Moore JK *et al.* 2010. Projected 21st century decrease in marine productivity: a multi-model analysis. *Biogeosciences* **7**: 979–1005.

Stoll MHC, Bakker K, Nobbe GH, Haese RR. 2001. Continous-flow analysis of dissolved inorganic carbon content in seawater. *Analytical Chemistry* **73**: 4111–4116.

Su W, Jakob T, Wilhelm C. 2012. The impact of nonphotochemical quenching of fluorescence on the photon balance in diatoms under dynamic light conditions. *Journal of Phycology* **48**: 336–346.

Suggett DJ, MacIntyre HL, Kana TM, Geider RJ. 2009. Comparing electron transport with gas exchange: parameterising exchange rates between alternative photosynthetic currencies for eukaryotic phytoplankton. *Aquatic Microbial Ecology* **56**: 147–162.

Takahashi T, Sutherland SC, Sweeney C, Poisson A, Metzl N, Tilbrook B, Bates N, Wanninkhof R, Feely RA, Sabine C *et al.* 2002. Global sea–air CO_2 flux based on climatological surface ocean pCO_2, and seasonal biological and temperature effects. *Deep Sea Research Part II: Topical Studies in Oceanography* **49**: 1601–1622.

Tatters AO, Roleda MY, Schnetzer A, Fu F, Hurd CL, Boyd PW, Caron DA, Lie AAY, Hoffmann LJ, Hutchins DA. 2013. Short- and long-term conditioning of a temperate marine diatom community to acidification and warming. *Philosophical Transactions of the Royal Society of London. Series B, Biological Sciences* **368**: 1627.

Tchernov D, Hassidim M, Luz B, Sukenik A, Reinhold L, Kaplan A. 1997. Sustained net CO_2 evolution during photosynthesis by marine microorganism. *Current Biology* **7**: 723–728.

Thamatrakoln K, Bailleul B, Brown CM, Gorbunov MY, Kustka AB, Frada M, Joliot PA, Falkowski PG, Bidle KD. 2013. Death-specific protein in a marine diatom regulates photosynthetic responses to iron and light availability. *Proceedings of the National Academy of Sciences, USA* **110**: 20123–20128.

Tortell PD. 2000. Evolutionary and ecological perspectives on carbon acquisition in phytoplankton. *Limnology and Oceanography* **45**: 744–750.

Tortell PD, Payne CD, Li Y, Trimborn S, Rost B, Smith WO, Riesselman C, Dunbar RB, Sedwick P, DiTullio GR. 2008. CO_2 sensitivity of Southern Ocean phytoplankton. *Geophysical Research Letters* **35**: L04605.

Trimborn S, Wolf-Gladrow D, Richter KU, Rost B. 2009. The effect of pCO_2 on carbon acquisition and intracellular assimilation in four marine diatoms. *Journal of Experimental Marine Biology and Ecology* **376**: 26–36.

Trimborn S, Brenneis T, Sweet E, Rost B. 2013. Sensitivity of Antarctic phytoplankton species to ocean acidification: growth carbon aquisition, and species interaction. *Limnology and Oceanography* **58**: 997–1007.

Trimborn S, Lundholm N, Thoms S, Richter K-U, Krock B, Hansen PJ, Rost B. 2008. Inorganic carbon acquisition in potentially toxic and non-toxic diatoms: the effect of pH-induced changes in seawater carbonate chemistry. *Physiologia Plantarum* **133**: 92–105.

Trimborn S, Thoms S, Petrou K, Kranz SA, Rost B. 2014. Photophysiological responses of Southern Ocean phytoplankton to changes in CO_2 concentrations: short-term versus acclimation effects. *Journal of Experimental Marine Biology and Ecology* **451**: 44–45.

Volk T, Hoffert MI. 1985. Ocean carbon pumps: analysis of relative strengths and efficiencies in ocean-driven atmospheric CO_2 changes. In: Sunquist ET, Broecker W, eds. *The carbon cycle and atmospheric CO_2: natural variation archean to present*. Washington, DC, USA: American Geophysical Union, Geophysical Monographs, 99–110.

Wagner H, Jakob T, Wilhelm C. 2006. Balancing the energy flow from captured light to biomass under fluctuating light conditions. *New Phytologist* **169**: 95–108.

Waring J, Klenell M, Bechtold U, Underwood GJC, Baker NR. 2010. Light-induced responses of oxygen photoreduction, reactive oxygen species

production and scavenging in two diatom species. *Journal of Phycology* **46**: 1206–1217.

Webb W, Newton M, Starr D. 1974. Carbon dioxide exchange of *Alnus rubra*. *Oecologia* **17**: 281–291.

Wu Y, Gao K, Riebesell U. 2010. CO_2-induced seawater acidification affects physiological performance of the marine diatom *Phaeodactylum tricornutum*. *Biogeosciences* **7**: 2915–2923.

Supporting Information

Additional supporting information may be found in the online version of this article.

Fig. S1 Night-time development of nonphotochemical quenching (NPQ) with increasing irradiance under the different treatment conditions.

Table S1 Results from two-way ANOVAs for all measured acclimation parameters

Table S2 Results from two-way ANOVAs for Chl fluorescence-based parameters, net primary production and the electron requirement for carbon fixation

Please note: Wiley Blackwell are not responsible for the content or functionality of any supporting information supplied by the authors. Any queries (other than missing material) should be directed to the *New Phytologist* Central Office.